Tenth International Conference on Computational Fluid Dynamics (ICCFD10), Barcelona, Spain, July 9-13, 2018

ICCFD10-207

Stability of Split-Form Flux-Reconstruction Schemes for Airfoil Flow Simulation with High-Order Mesh

T. Watanabe[1], Y. Abe[2], T. Haga[3], R. Takaki[4], A. Oyama[4],
T. Nonomura[5] and K. Miyaji[1]
Corresponding author: watanabe-takara-sc@ynu.jp

[1] Yokohama National University, Japan
[2] Imperial College London, UK
[3] Research Unit III, JAXA, Japan
[4] Institute of Space and Astronautical Science, JAXA, Japan
[5] Tohoku University, Japan

Abstract: This paper discusses numerical stability of the split-form FR scheme for a practical flow simulation involving wall boundary condition and high-order curved mesh, i.e., laminar flow simulation of the NACA0012 airfoil. Numerical stability of FR schemes in divergence form and FR schemes in split form is compared by investigating the allowable maximum time step width. The results show that the computation using the split-form FR schemes is stable whereas the computation using the divergence-form FR schemes blow up in the most conditions. This study also shows that the FR scheme in divergence form with the eighth-order solution approximation on a GP4 mesh works well for a practical flow simulation.
Keywords: Flux Reconstruction Scheme, High-Order Scheme, Numerical Stability

1 Introduction

There are engineering demands for quick and accurate simulation of turbulent flows around complex geometries such as an airplane or a rocket. For that purpose, high-order unstructured schemes have been extensively studied.

However, high-order schemes have a problem of numerical instability caused by accumulation of the aliasing errors that originates from the discretization of the nonlinear convective term. As a remedy for the problem, it is known that split forms (also known as (pseudo) skew-symmetric forms) of the convection terms can reduce the aliasing errors and preserve the kinetic energy. Gassner [1] has developed split-form discontinuous Galerkin (DG) schemes in the context of kinetic energy preservation (KEP), which has been later extended to the flux reconstruction (FR) schemes (split-form FR schemes, hereinafter) by deriving more rigorous conditions [2]. So far, applications of split-form FR schemes have been limited to simple flow simulations such as periodic turbulent flows on Cartesian mesh. Thus, the robustness of the split-form FR schemes has not yet been adequately investigated for more practical flow computations involving wall boundary conditions and high-order curved meshes.

In this study, split-form FR schemes in [3] are focused because of their relatively lower computational cost among the high-order unstructured schemes. We start with a simulation of laminar flows over the NACA0012 airfoil as a first step of simulation of practical flows by split-form FR schemes. Stability of the scheme are verified in the simulations with a curved wall at eighth-order (P7) approximation of solution. Numerical stability of the split-form FR is compared with the divergence-form (i.e. conservation-form) FR schemes.

2 Approach

Numerical stability of a split-form FR scheme is compared with that in the divergence form. Simulations of laminar flow over the NACA0012 airfoil are conducted in six flow conditions with high angles of attack. The flow conditions are presented in Table 1. Here, Mach number and angle of attack are changed while Reynold number based on the airfoil chord length is fixed to 5,000.

Table 1: Conditions for laminar flow over the NACA0012 Airfoil.

Condition	Mach number	Angle of attack	Reynolds number
M05A08	0.5	8	5,000
M05A09	0.5	9	5,000
M05A10	0.5	10	5,000
M05A11	0.5	11	5,000
M04A10	0.4	10	5,000
M06A10	0.6	10	5,000

In this study, the third-order Total-variation-diminishing Runge-Kutta scheme for time-marching method, SLAU flux [4] for common flux, Bassi and Rebay (BR2) [5] flux for viscous flux are used. The Gauss-Lobatto points are adopted as the solution points because the sufficient condition for the primary conservation of the split-form FR schemes is to adopt the Gauss-Lobatto solution points. For metric evaluation, non-conservative form is used. The sufficient conditions for the kinetic energy preservation are to adopt a kinetic energy preserving flux and the g_2 correction function. While there are some ways to express split forms, the form [6] shown as eq (1) is used.

$$(\mathrm{Split}_{\mathrm{Fe}}) \coloneqq \frac{1}{2}\frac{\partial}{\partial \xi}\left(\rho \hat{\mathrm{U}} \phi\right) + \frac{1}{2}\phi\frac{\partial}{\partial \xi}\left(\rho \hat{\mathrm{U}}\right) + \frac{1}{2}\rho \hat{\mathrm{U}}\frac{\partial}{\partial \xi}(\phi) \tag{1}$$

C-type topology grids are generated where the number of cells is 864 for P7 and 3,600 for P3, respectively. For accurate representation of the curved wall, high-order meshes are used. For coordinate transformation, quadratic shape functions are used.

In general, the numerical stability of schemes can be investigated by von Neumann stability analysis when the equation under consideration is linear. However, it is difficult to investigate split-form FR schemes using von Neumann stability analysis because they are nonlinear. In order to investigate numerical stability of the split-form FR schemes, the following approach is adopted.

(1) Search for the maximum time-step width which allows stable computation up to non-dimensional time of 50 using FR scheme in split-form.

(2) Check if computation is stable up to non-dimensional time of 50 using FR scheme in divergence form with the maximum time-step width found in step (1).

(3) If computation blow up in (2), check if computation is stable up to non-dimensional time of 50 using FR scheme in divergence form with half of the maximum time-step width found in step (1).

3 Result

3.1 Robustness of Split-Form FR Schemes

Results of stability analysis are presented in Tables 2 and 3. Table 2 and 3 shows the maximum time-step width which allows stable computation up to non-dimensional time of 50 using FR scheme in the split form. The symbol "✓" represents that the computation using FR scheme in divergence form is stable up to non-dimensional time of 50. These tables show that the split-form FR schemes are stable for the practical flow simulation, i.e., laminar flow simulation of the NACA0012 airfoil. As for the FR scheme in divergence form, the computation is unstable in most of the conditions even when the time step size becomes half.

Table 2: Maximum time-step width (angle of attack is changed).

condition	Correction Function	Polynomial of order	Maximum time step of split form	Divergence form	
				Same time step	Half time step
M05A08	g_{Ga}	7	0.99×10^{-4}	Blow up	Blow up
M05A08	g_{Ga}	3	1.80×10^{-4}	✓	✓
M05A08	g_2	7	1.01×10^{-4}	Blow up	Blow up
M05A08	g_2	3	1.95×10^{-4}	✓	✓
M05A09	g_{Ga}	7	0.92×10^{-4}	Blow up	Blow up
M05A09	g_{Ga}	3	1.62×10^{-4}	Blow up	Blow up
M05A09	g_2	7	0.94×10^{-4}	Blow up	Blow up
M05A09	g_2	3	1.85×10^{-4}	Blow up	Blow up
M05A10	g_{Ga}	7	0.84×10^{-4}	Blow up	Blow up
M05A10	g_{Ga}	3	1.63×10^{-4}	Blow up	Blow up
M05A10	g_2	7	0.88×10^{-4}	Blow up	Blow up
M05A10	g_2	3	1.75×10^{-4}	Blow up	Blow up
M05A11	g_{Ga}	3	1.54×10^{-4}	Blow up	Blow up
M05A11	g_2	3	1.66×10^{-4}	Blow up	Blow up

Table 3: Maximum time-step width (Mach number is changed).

Condition	Correction Function	Polynomial of order	Maximum time step of split form	Divergence form	
				Same time step	Half time step
M04A10	g_{Ga}	7	1.26×10^{-4}	Blow up	Blow up
M04A10	g_{Ga}	3	2.36×10^{-4}	Blow up	Blow up
M04A10	g_2	7	1.29×10^{-4}	Blow up	Blow up
M04A10	g_2	3	2.57×10^{-4}	Blow up	Blow up
M05A10	g_{Ga}	7	0.84×10^{-4}	Blow up	Blow up
M05A10	g_{Ga}	3	1.63×10^{-4}	Blow up	Blow up
M05A10	g_2	7	0.88×10^{-4}	Blow up	Blow up
M05A10	g_2	3	1.75×10^{-4}	Blow up	Blow up
M06A10	g_{Ga}	3	1.03×10^{-4}	Blow up	Blow up
M06A10	g_2	3	1.11×10^{-4}	Blow up	Blow up

The convergence history of the condition M05A10 (Mach number of 0.5 and angle of attack of 10 degrees) is shown in Figure 1. Computations are conducted under the same time-step width, i.e., the allowable maximum time-step width for the split-form FR scheme. The computation using split-form FR scheme is stable whereas the divergence form diverges early. Stable characteristic of the split-form FR schemes is probably due to the reduction in aliasing error. The present computation also shows that computation with eighth-order (P7) solution approximation is possible for practical aerodynamic simulation with a curved wall.

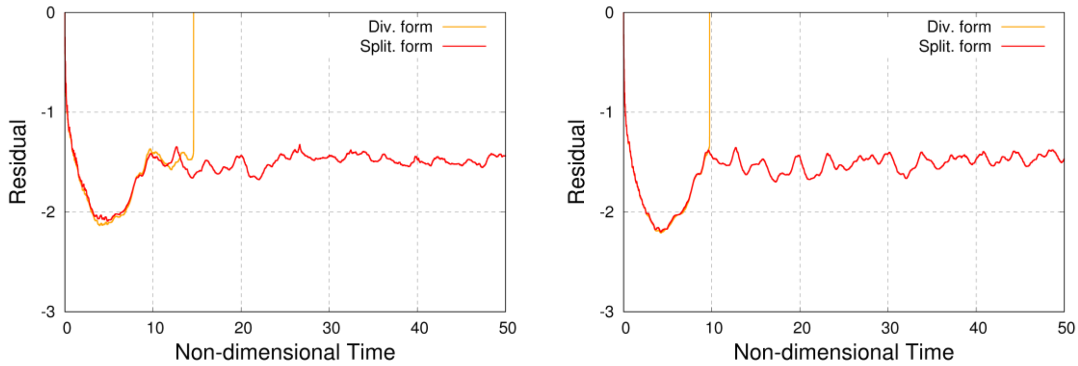

(a) eighth-order computation (P7) (b) fourth-order computation (P3)

Figure 1: Comparison of convergence histories for condition M05A10.

Table 2 shows that the maximum time-step width of the g_2 correction function is also larger than that of g_{Ga} correction function for the split-form FR schemes. The difference between the g_2 correction function and the g_{Ga} correction function in the maximum time step width probably comes from the difference in the slope of the function. It is known that steeper correction function results in a scheme with a smaller CFL limit and that the g_2 correction function is less steep than the g_{Ga} correction function.

3.2 Computation on High-Order Mesh

Now we investigate effect of high-order mech. High-order mesh enables accurate curved wall representation. We use two types of high-order meshes: GP2 mesh (quadratic shape functions are used) and GP4 mesh (quartic shape functions are used). The number of cells is 864 and the airfoil is composed of 32 faces. Using these meshes, laminar flow over the NACA0012 airfoil is computed with the eighth-order solution approximation. The flow condition is Mach number of 0.8, angle of attack of 10 degrees, and Reynolds number of 500. The TC-PGS scheme [7] for time-marching method and SLAU flux for common flux are used. The Gauss points are adopted for solution points. Here the FR scheme in divergence form is used for convection term.

Figure 2 shows surface pressure coefficient distributions obtained by computation with GP4 mesh and GP2 mesh. The result is compared with surface pressure coefficient distribution in [8]. This result shows that the surface pressure coefficient distribution of GP4 mesh are accurate but the surace pressure coefficient distribution obtained on the GP2 mesh is different from the reference data especially on the upper surface and in the trailing edge.

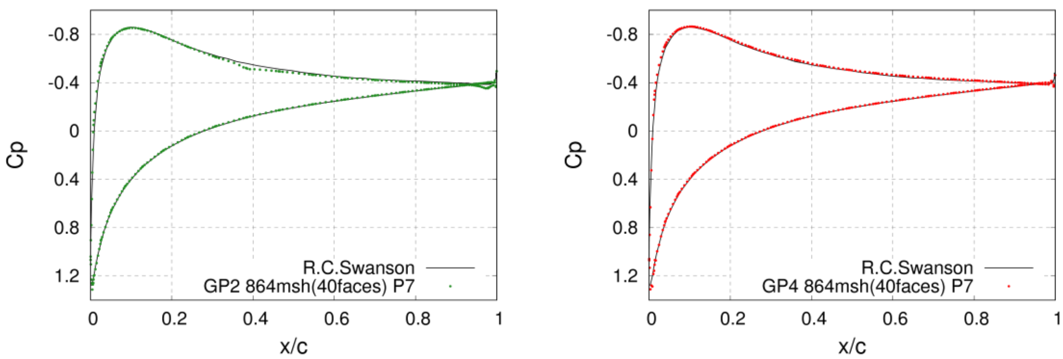

(a) C_p distribution on GP2 mech (b) C_p distribution on GP4 mesh

Figure 2: Comparison of surface pressure coefficient distributions.

4 Concluding Remarks

This paper discussed numerical stability of the split-form FR scheme for a practical flow simulation involving wall boundary condition and high-order curved mesh, i.e., laminar flow simulation of the NACA0012 airfoil. Numerical stability of FR schemes in divergence form and FR schemes in split form was compared by investigating the allowable maximum time step width. The results showed that the computation using the split-form FR schemes is stable whereas the computation using the divergence-form FR schemes blow up in the most conditions. This study also showed that the FR scheme in divergence form with the eighth-order solution approximation on a GP4 mesh works well for a practical flow simulation.

References

[1] G.J. Gassner. A kinetic energy preserving nodal discontinuous Galerkin spectral element method. Int. J. Numer. Methods Fluids, 76, 28–50, 2014.

[2] H.T. Huynh. A flux reconstruction approach to high-order schemes including discontinuous Galerkin methods. AIAA 2007-4079, 2007.

[3] Y. Abe, I. Morinaka, T. Haga, T. Nonomura, H. Shibata and K. Miyaji. Stable, non-dissipative, and conservative flux-reconstruction schemes in split forms. J. Comput. Phys. 353, 193-227, 2018.

[4] E. Shima and K. Kitamura. On New Simple Low-Dissipation Scheme of AUSM-Family for All Speeds, AIAA Paper 2009-136, 2009.

[5] F. Bassi and S. Rebay. Numerical evaluation of two discontinuous Galerkin methods for the compressible Navier-Stokes equations. Int. J. Numer. Meth. Fluids, 197-207, 2002.

[6] W.J. Feiereisen, W.C. Reynolds and J.H. Ferziger. Numerical simulation of a compressible homogeneous, turbulent shear flow. Technical report, Report TF-13, Standard University, No.9, 1981.

[7] T. Haga and E. Shima. Matrix-free defect correction scheme for implicit high-order flux reconstruction solver (in Japanese), in proceedings of the symposium on computational fluid dynamics, B05-3, 2015.

[8] R. Swanson and S. Langer. Comparison of NACA 0012 Laminar Flow Solutions: Structured and Unstructured Grid Methods. NASA/TM-2016-219003, 2016